High-temperature phases of $SrRuO_3$

Brendan J. Kennedy
School of Chemistry, The University of Sydney, Sydney, NSW 2006, Australia

Brett A. Hunter
Australian Nuclear Science and Technology Organisation, PMB 1, Menai, NSW 2234, Australia

(Received 1 December 1997)

The crystal structure of $SrRuO_3$ at high temperatures has been studied using powder neutron diffraction and the Rietveld method. It was determined that from 300 K to approximately 820 K the structure of $SrRuO_3$ is orthorhombic ($Pbnm$). The material then undergoes a phase transition and becomes tetragonal ($I4/mcm$) between ~820 and 920 K. The high-temperature (>920 K) structure was found to be the standard cubic perovskite ($Pm3m$). From the neutron-diffraction data and the space group assignments, the orthorhombic to tetragonal phase transition must be first order, while the transition from the tetragonal to cubic phase is consistent with a second-order phase transition.
[S0163-1829(98)05425-3]

I. INTRODUCTION

The structural and electronic properties of mixed Sr-Ru oxides are of considerable current interest, with the recent reports of superconductivity in Sr_2RuO_4 and $Sr_2YRu_{1-x}Cu_xO_9$ systems[1,2] and of a temperature-dependent metal-insulator transition in $Sr_3Ru_2O_7$.[3] The parent perovskite compound $SrRuO_3$ has been studied for over 30 years,[4,5] and is a rare example of a ferromagnetic $4d$ oxide with a sizable magnetic moment, being about one Bohr magneton per formula unit. At room temperature the structure of $SrRuO_3$, like that of many ABO_3 perovskite compounds, exhibits orthorhombic $Pbnm$ symmetry, and a high-resolution powder neutron-diffraction study demonstrated it to be isostructural with $GdFeO_3$.[6,7] The degree of distortion of these perovskites may be described by tilting of the BO_6 octahedra,[8,9] where these tilts are usually used as order parameter(s) in describing any phase transitions. Typically the degree of the orthorhombic distortion decreases with increasing temperature, and the structure transforms to other perovskite-type structures, such as observed in the oxides $CaTiO_3$ (Ref. 10) and $SrZrO_3$.[11] The purpose of the present paper is to report data on the evolution of the crystal structure of $SrRuO_3$ at high temperatures by powder neutron diffraction and the Rietveld method.

II. EXPERIMENT

Powder samples of $SrRuO_3$ were synthesized by the solid-state reaction of stoichiometric quantities of RuO_2 (Aldrich, 99.9%) and $SrCO_3$ (Aldrich, 99.995%). The homogeneous mixtures were compressed into 13-mm pellets, and fired in air at 800 °C for 12 h, and then at 1200 °C, with periodic regrinding and pressing until the reaction was complete. The room-temperature powder x-ray-diffraction pattern recorded on a Siemens D-5000 diffractometer using Cu-K_α radiation showed the material had orthorhombic symmetry, consistent with $Pbnm$ symmetry with no detectable impurities. The powder neutron-diffraction patterns were recorded using a wavelength of 1.4928(3) Å, in 0.05° steps over the range $0°<2\theta<154°$ on the 24 detector high-resolution powder diffractometer[12] on the HIFAR reactor operated by the Australian Nuclear Science and Technology Organisation. The lightly ground sample (~10 g) was contained in a thin-walled 12-mm diameter stainless-steel can. The data were collected at nine different temperatures between 573 and 1023 K with the sample chamber open to the atmosphere. The structural refinements were undertaken using a modified version of the Rietveld program LHPM.[13,14] The background was defined by a third-order polynomial in 2θ, and was refined simultaneously with the other profile parameters. A Voigt function was used to describe the neutron-diffraction peak shape, where the Gaussian width component varied as $\mathcal{F}^2 = U\tan^2\theta + V\tan\theta + W$, and the width of Lorentzian component was varied as $\eta\sec\theta$ to model particle size. The coherent neutron-scattering lengths used were Ru = 0.721, Sr = 0.702, and $O = 0.5803$ fm (10^{-15} m). The 2θ region corresponding to a peak from the furnace near 24° was excluded from the refinements. An additional Fe phase was used in the refinement process to account for the stainless-steel can.

III. RESULTS AND DISCUSSION

The powder neutron-diffraction data showed a sequence of phase transitions from orthorhombic to tetragonal and then to cubic as the temperature increased, where the tetragonal phases exists over a narrow temperature range from about 820 to 920 K. The variations of the cell parameters are shown in Fig. 1. For the orthorhombic phase the three cell edges increase linearly with temperature with the rate of change of the b axis being larger than that of the a axis. These changes are consistent with the behavior of other $Pbnm$ perovskites such as $CaTiO_3$ (Ref. 10) and $MgSiO_3$.[15]

A. Orthorhombic structure

The room-temperature powder x-ray-diffraction pattern of $SrRuO_3$ was analyzed in terms of the orthorhombic $\sqrt{2}a_p$

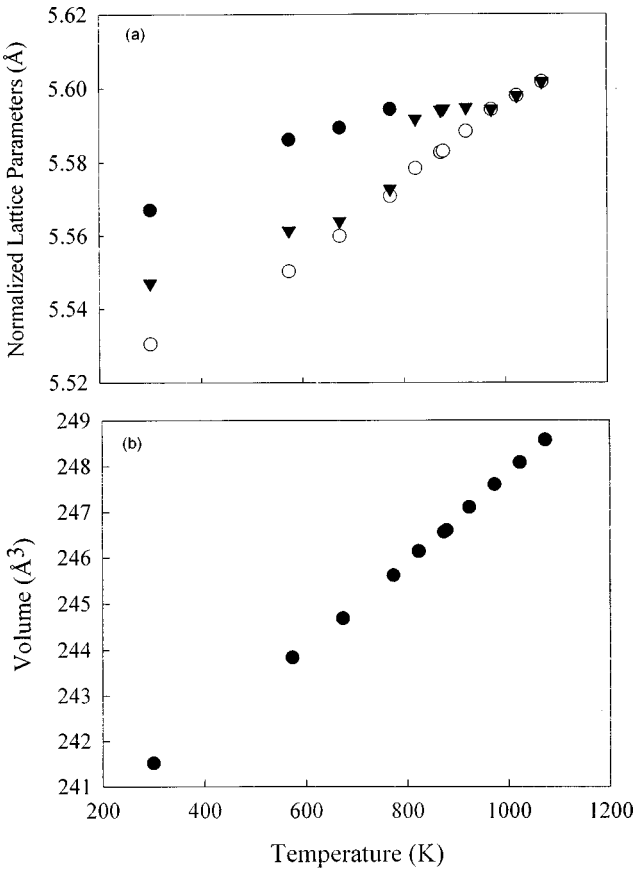

FIG. 1. Temperature dependence of the (a) normalized lattice parameters and (b) volume. a: lattice parameter (●); b: lattice parameter (○); and c: lattice parameter (▼). Values for the 300-K data points were taken from Ref. 7.

$\times\sqrt{2}a_p\times 2a_p$ cell, where a_p is the cell length of the cubic unit cell, as described by Jones *et al.*[7] An orthorhombic cell is typically observed when the A-O bond length is less than $\sqrt{2}$ times the B-O bond length. This results in rotations of the BO_6 octahedra. For the $Pbnm$ space group this is described as counterclockwise rotations of equivalent magnitude about the $[010]_{\text{cubic}}$ and $[001]_{\text{cubic}}$ directions, and a clockwise rotation about the $[100]_{\text{cubic}}$ direction. In the Glazer notation,[8] this is $b^-b^-a^+$. O'Keeffe and Hyde[16] found that in the limit of small rotations about ⟨111⟩, the octahedra distortion in $Pbnm$ can be described by a single rotation angle, φ_o. Even though symmetry allows the rotation axis to itself be tilted, as an approximation the single rotation angle is a good descriptor.

Powder neutron-diffraction data were collected at 573, 673 and 773 K. Initially, refinements using isotropic thermal parameters were performed, but the measures of fit remained high. Using anisotropic thermal parameters resulted in noticeably better fits, although the value for B_{33} of the Ru cation was always negative. Since it is necessary to use six parameters to describe the thermal parameters for Ru, and previous studies of orthorhombic perovskites have indicated that the thermal ellipsoid of the B-type cation is approximately spherical,[7] an isotropic thermal parameter was used for the Ru cation in the final refinements. Allowing the occupations to vary suggested the sample to contained approximately 8% Ru vacancies. An identical result, within the estimated errors, was found in all the refinements from the data collected at the various temperatures, demonstrating this to be a feature of the sample. The origin of the Ru vacancies is unclear, although the alumina crucible used to prepare the sample was discolored after the reaction. The final refinement, including the Ru vacancies, is shown in Fig. 2.

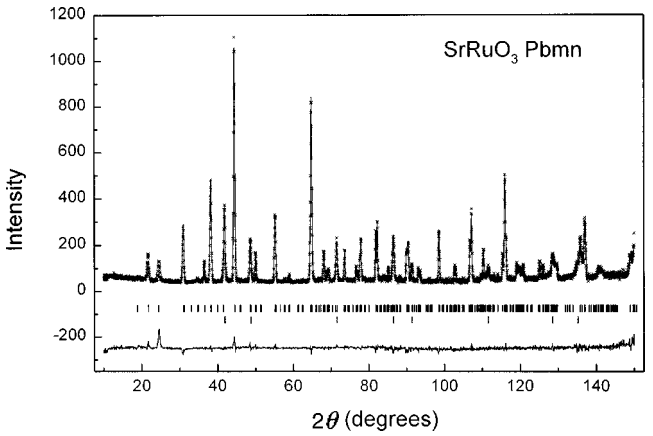

FIG. 2. Observed, calculated, and difference powder neutron-diffraction profiles for orthorhombic $SrRuO_3$ at 573 K. The upper set of small vertical makers show the positions of all the allowed Bragg reflections for $SrRuO_3$ while the lower set is for Fe from the sample holder.

A second feature of the refinement is the larger than expected estimated standard deviations in some of the positional parameters (Table I). By examination of the structure this can be explained by the large, and highly, anisotropic thermal displacement parameters. The correlation coefficients from the refinement process suggest the same.

B. Tetragonal structure

The powder neutron pattern of $SrRuO_3$ at 823 K is shown in Fig. 3. It is clear from the pattern that a number of superlattice lines associated with titled octahedra and displaced cations are present. Initial refinements using the orthorhombic structure suggested the cell was pseudotetragonal; however, a satisfactory fit could not be obtained. Examination of the data showed that the splitting of the $(516)_{\text{ortho}}$ and $(156)_{\text{ortho}}$ reflections near $2\theta=125°$ characteristic of the orthorhombic structure were absent (Fig. 4), suggesting tetragonal symmetry. The space group $I4/mcm$ was identified as the most probable, this being found in $SrZrO_3$ at 1173 K,[11] and in $SrTiO_3$ below 110 K.[17]

This is a one-tilt system described by Glazer as $a^0a^0c^-$, where the octahedra are rotated around the $[001]_{\text{cubic}}$ direction. As the octahedra are not coupled in the c direction, adjoining layers of octahedra can be either in phase or out of phase, as denoted by c^+ or c^- respectively. The neutron data clearly show evidence of the c doubling inherit from the out-of-phase octahedra rotations. The lattice is characterized by a $\sqrt{2}a_p\times\sqrt{2}a_p\times 2a_p$ cell (a_p is the cubic lattice parameter), and the octahedra distortion by a single rotation angle φ_l.

In the $I4/mcm$ space group, the Sr occupies the $4b$ site at $(0,\frac{1}{2},\frac{1}{4})$ and the Ru a $4c$ site at (0,0,0). There are two types of oxygen atoms, O(1) at a $4a$ site at $(0,0,\frac{1}{4})$ and O(2) at an $8h$

TABLE I. Structural parameters and selected bond lengths and angles of orthorhombic $SrRuO_3$ from neutron powder diffraction. The Rietveld refinements were done in the $Pbnm$ space group (No. 62). The atom positions are Sr $4c(x,y,\frac{1}{4})$, Ru $4b(0,0,\frac{1}{2})$, O1 $4c(x,y,\frac{1}{4})$, and O2 $8d(x,y,z)$. The numbers in parentheses are the estimated standard deviations in the last significant digit. The rotation angle φ_0 is calculated from $\varphi_0=\tan^{-1}[z(\mathrm{O2})Sqrt(48)]$ (Ref. 16).

T (K)		573 K	673 K	773 K
a (Å)		5.5861(1)	5.5893(2)	5.5943(1)
b (Å)		5.5502(1)	5.5599(2)	5.5708(1)
c (Å)		7.8650(2)	7.8686(2)	7.8810(2)
V (Å^3)		243.84(1)	244.69(1)	245.61(1)
Sr	x	0.0003(8)	0.0008(8)	0.0009(9)
	y	0.0130(9)	−0.0027(19)	−0.0001(27)
	B (Å^2)	0.93(3)	1.36(3)	1.59(3)
Ru	n	0.94(1)	0.96(1)	0.93(1)
	B (Å^2)	0.03(3)	0.14(3)	0.05(3)
O1	x	0.0482(7)	0.0452(6)	0.0407(7)
	y	0.4985(13)	0.4938(26)	0.4977(37)
	B (Å^2)	0.97(6)	1.37(3)	1.55(7)
O2	x	0.2695(5)	0.2518(26)	0.2512(22)
	y	0.2697(5)	0.2477(26)	0.2509(26)
	z	0.0235(4)	0.0220(4)	0.0190(4)
	B (Å^2)	1.01(4)	1.72(5)	2.04(5)
φ_0 (deg)		9.25	8.67	7.50
Ru-O1 (Å)		1.985	1.984	1.983
Ru-O2 (Å)		1.984	1.995	1.981
Ru-O2 (Å)		1.983	1.962	1.978
Ru-O1-Ru (deg)		164.40	165.23	166.80
Ru-O2-Ru (deg)		166.05	169.96	171.31
O1-Ru-O2 (deg)		90.06	90.48	90.10
O1-Ru-O2 (deg)		90.46	90.85	90.58
O2-Ru-O2 (deg)		90.86	90.74	90.57
R_{Bragg} (%)		3.64	3.98	3.66
R_p (%)		6.51	5.74	4.73
R_{wp} (%)		7.84	7.12	5.80
χ^2 (%)		2.50	2.21	3.04

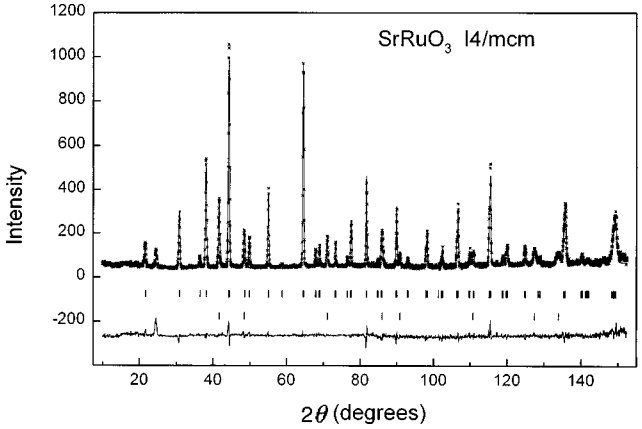

FIG. 3. Observed, calculated, and difference powder neutron-diffraction profiles for tetragonal $SrRuO_3$ at 823 K. The upper set of small vertical makers show the positions of all the allowed Bragg reflections for $SrRuO_3$ while the lower set is for Fe from the sample holder.

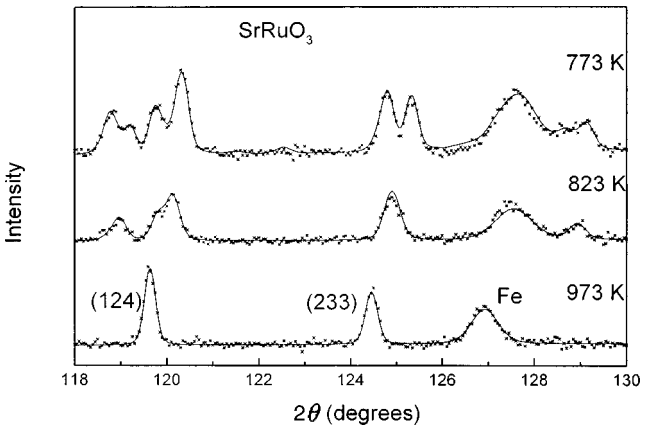

FIG. 4. Part of the powder neutron-diffraction profiles showing the temperature dependence of some of the superlattice reflections associated with tilted octahedra and displaced cations. The broad peak near 127° is from the Fe sample holder.

TABLE II. Structural parameters and selected bond lengths and angles of tetragonal $SrRuO_3$ from neutron powder diffraction. The Rietveld refinements were done in the $I4/mcm$ space group (No. 140). The atom positions are Sr $4b(0,\frac{1}{2},\frac{1}{4})$, Ru $4c(0,0,0)$, O1 $4a(0,0,\frac{1}{4})$, and O2 $8h(\frac{1}{4}+u,\frac{3}{4}+u,0)$. The numbers in parentheses are the estimated standard deviations in the last significant digit. The rotation angle φ_t is calculated from $\varphi_t \sim 2\tan^{-1}(2u)$.

T (K)		823 K	873 K	878 K	923 K
a (Å)		5.5784(2)	5.5827(2)	5.5830(1)	5.5884(1)
c (Å)		7.9078(3)	7.9111(3)	7.9115(2)	7.9121(3)
V (Å^3)		246.14(1)	246.56(1)	246.60(1)	247.10(1)
Sr	B_{11} (Å^2)	0.67(6)	0.96(8)	0.89(6)	0.85(8)
	B_{33} (Å^2)	0.94(6)	0.79(7)	0.80(5)	1.01(8)
Ru	n	0.92(1)	0.92(1)	0.91(1)	0.91(1)
	B_{11} (Å^2)	0.15(6)	0.42(8)	0.41(6)	0.08(8)
	B_{33} (Å^2)	0.53(6)	0.35(7)	0.32(6)	0.72(9)
O1	u	0.0255(4)	0.0230(6)	0.0233(4)	0.0199(5)
	B_{11} (Å^2)	2.2(2)	2.5(2)	2.5(2)	2.5(2)
	B_{33} (Å^2)	0.33(6)	0.34(8)	0.33(7)	0.13(8)
O2	B_{11} (Å^2)	0.75(6)	1.28(9)	1.13(6)	1.35(9)
	B_{33} (Å^2)	1.89(8)	1.65(9)	1.65(7)	1.93(11)
	B_{13} (Å^2)	0.39(8)	1.12(11)	1.07(9)	1.01(7)
φ_t (deg)		5.84	5.27	5.34	4.56
Ru-O1 (Å)		1.977	1.978	1.978	1.978
Ru-O2 (Å)		1.983	1.982	1.982	1.982
Ru-O1-Ru (deg)		168.35	169.49	169.35	170.90
R_{Bragg} (%)		3.48	2.48	3.06	2.92
R_p (%)		7.47	7.36	6.14	5.89
R_{wp} (%)		8.61	8.99	7.45	7.30
χ^2 (%)		2.70	1.82	2.39	2.29

site at $(\frac{1}{4}+u,\frac{3}{4}+u,0)$. Refinement in the $I4/mcm$ space group clearly showed this model to better describe the structure compared to the orthorhombic structure. Appreciably better agreement between the observed and calculated profiles was obtained when anisotropic thermal parameters were employed, and the occupancy of the Ru site was refined. The final refined parameters and measures of fit are given in Table II.

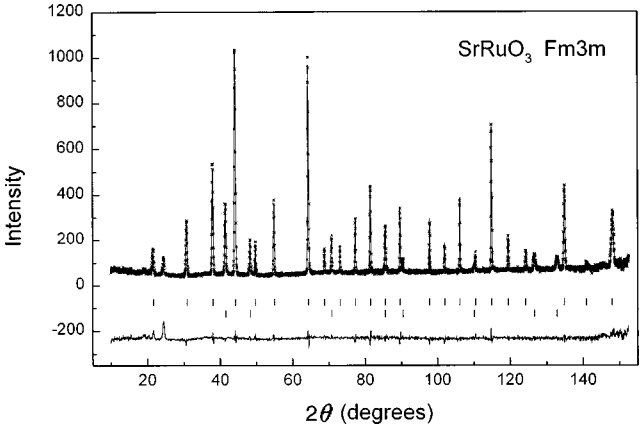

FIG. 5. Observed, calculated, and difference powder neutron-diffraction profiles for cubic $SrRuO_3$ at 1023 K. The upper set of small vertical makers show the positions of all the allowed Bragg reflections for $SrRuO_3$, while the lower set is for Fe from the sample holder.

C. Cubic structure

The diffraction patterns collected above 973 K do not show evidence of any superlattice reflections (Figs. 3 and 5), and consequently the structure was refined in the standard cubic perovskite space group $Pm3m$. The Ru occupies the

TABLE III. Structural parameters and selected bond lengths of cubic $SrRuO_3$ from neutron powder diffraction. The Rietveld refinements were done in the $Pm3m$ space group (No. 221). The atom positions are Sr $1b(\frac{1}{2},\frac{1}{2},\frac{1}{2})$, Ru $1a(0,0,0)$ and O1 $3d(\frac{1}{2},0,0)$. The numbers in parentheses are the estimated standard deviations in the last significant digit.

T (K)		973 K	1023 K	1073 K
a (Å)		3.9557(1)	3.9583(1)	3.9609(1)
V (Å^3)		61.899(2)	62.019(2)	62.142(3)
Sr	B (Å^2)	2.60(5)	2.90(5)	3.16(7)
Ru	n	0.92(1)	0.91(1)	0.91(1)
	B (Å^2)	1.06(4)	1.15(4)	1.32(6)
O1	B_{11}	0.80(9)	0.86(9)	0.91(13)
	B_{22} (Å^2)	6.64(9)	6.80(9)	6.85(13)
Ru-O1 (Å)		1.978	1.979	1.981
R_{Bragg} (%)		2.56	2.32	2.67
R_p (%)		6.16	6.43	8.62
R_{wp} (%)		7.62	7.69	10.72
χ^2 (%)		2.48	2.44	1.84

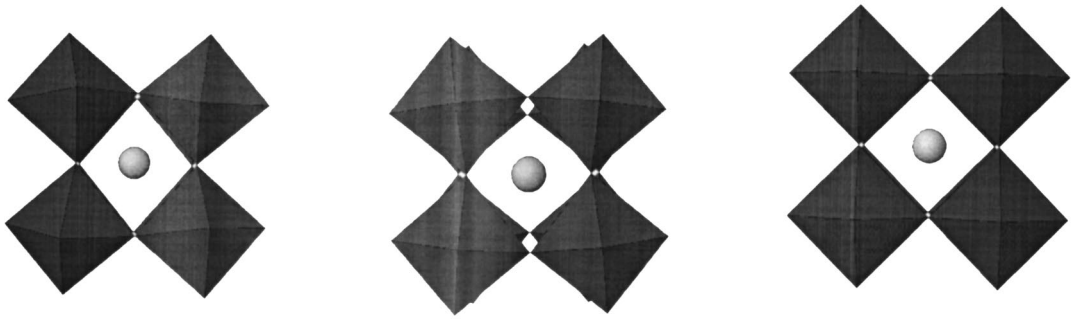

FIG. 6. View of the orthorhombic, tetragonal, and cubic forms of $SrRuO_3$, illustrating the tilting of the RuO_6 octahedra. In all cases the cycle represents the Sr atoms.

$1a$ site at (0,0,0), the Sr the $1b$ site at $(\frac{1}{2},\frac{1}{2},\frac{1}{2})$, and the O the $3d$ site at $(0,0,\frac{1}{2})$. Similar to the low-temperature phase refinements, it was found that considerably better refinements were obtained using anisotropic, rather than isotropic thermal parameters. For example, the refinement indicator χ^2 for the 973-K data decreased from 4.03% to 2.74%, and R_{Bragg} from 7.51% to 3.64% when anisotropic thermal parameters were used. As evident from Fig. 5, the use of anisotropic thermal parameters and variable Ru occupancy leads to a good agreement between the observed and calculated diffraction profiles.

D. Phase transitions

Despite the widespread occurrence of perovskite-type oxides there, are relatively few detailed studies of the high-temperature phase transitions available. Noticeable exceptions include, the early work of Ahtee, Glazev, and Hewal,[11] and the recent study of $CaTiO_3$ by Vogt and Schmahl.[18]

The tetragonal space group $I4/mcm$ is a subgroup of the cubic space group $Pm3m$, and from Stokes and Hatch[19] can be obtained by a continuous ferroelastic second-order phase transition (although it is not required to be). The irreducible representation that drives the phase transition is $R4^+$, and physically represents the out-of-phase rotation in the $[001]_{\mathrm{cubic}}$ direction. This can be described by a single order parameter, say, the angle of rotation. The neutron-scattering data presented here are consistent with a second-order phase transition, as has been observed in similar systems.[11]

In contrast, although $Pbnm$ is a subgroup of $Pm3m$, it is not a subgroup of $I4/mcm$. This means that the tetragonal-orthorhombic phase transition is required to be first order based on symmetry considerations. The neutron data do show a small discontinuous change in the a lattice parameter, although as is clear from Fig. 1 that there is not corresponding discontinuous change in volume.

IV. CONCLUSIONS

The high-temperature phases of $SrRuO_3$ were studied using neutron powder diffraction (see Fig. 6 and Table III). It was found that the orthorhombic phase, found at 300 K, persists up until 800 K, where it transforms via a first-order phase transition into a tetragonal phase. This tetragonal phase persists until approximately 950 K, where it transforms via a second-order transition to the standard cubic perovskite structure

$$\text{orthorhombic} \xrightarrow[820\ \mathrm{K}]{} \text{tetragonal} \xrightarrow[950\ \mathrm{K}]{} \text{cubic},$$

This study clearly demonstrates the ability of powder neutron diffraction, coupled with theoretical analysis, to monitor and understand the high-temperature phase transitions in perovskite-type oxides.

ACKNOWLEDGMENTS

B.J.K. thanks the Australian Institute for Nuclear Science and Technology (AINSE) for their support of this work, and Dr. Bryan Chakoumakos (ORNL) for informing us of his unpublished studies on $SrRuO_3$. B.A.H. wishes to thank Dr. C. J. Howard (ANSTO) for many useful discussions.

[1] Y. Maeno, H. Hashimoto, K. Yoshida, S. Nishizaki, T. Fujita, J. G. Bednorz, and L. Lichtenberg, Nature (London) **372**, 532 (1994).
[2] M. K. Wu, D. Y. Chen, F. Z. Chien, S. R. Sheen, D. C. Ling, C. Y. Tai, G. Y. Tseng, D. H. Chen, and F. C. Zhang, Z. Phys. B **102**, 37 (1997).
[3] S. Ikeda, Y. Maeno, M. Nohara, and T. Fujita, Physica C **263**, 558 (1996).
[4] J. J. Randall and R. Ward, J. Am. Chem. Soc. **81**, 2629 (1959).
[5] A. Callaghan, C. W. Moeller, and R. Ward, Inorg. Chem. **5**, 1572 (1966).
[6] R. J. Bouchard and J. L. Gillson, Mater. Res. Bull. **7**, 873 (1972).
[7] C. W. Jones, P. D. Battle, P. Lightfoot, and T. A. Harrison, Acta Crystallogr., Sect. C: Cryst. Struct. Commun. **45**, 365 (1989).
[8] A. M. Glazer, Acta Crystallogr., Sect. B: Struct. Crystallogr. Cryst. Chem. **28**, 3384 (1972).
[9] P. M. Woodward, Acta Crystallogr., Sect. B: Struct. Sci. **53**, 32 (1997).
[10] X. Liu and R. C. Liebermann, Phys. Chem. Miner. **20**, 171 (1993).
[11] M. Ahtee, A. M. Glazer, and A. W. Hewat, Acta Crystallogr., Sect. B: Struct. Crystallogr. Cryst. Chem. **34**, 752 (1978).
[12] C. J. Howard, C. J. Ball, R. L. Davis, and M. M. Elcombe, Aust. J. Phys. **36**, 507 (1983).

[13] B. A. Hunter (unpublished).
[14] R. J. Hill and C. J. Howard (AAEC, Lucas Heights, NSW, 1986).
[15] N. L. Ross and R. M. Hazen, Phys. Chem. Miner. **16**, 415 (1989).
[16] M. O'Keeffe and B. G. Hyde, Acta Crystallogr., Sect. B: Struct. Crystallogr. Cryst. Chem. **33**, 3802 (1977).
[17] J. Unoki and T. Sakudo, J. Phys. Soc. Jpn. **23**, 546 (1967).
[18] T. Vogt and W. W. Schmahl, Europhys. Lett. **24**, 281 (1993).
[19] H. T. Stokes and D. M. Hatch, *Isotropy Subgroups of the 230 Crystallographic Space Groups* (World Scientific, Singapore, 1988).